

On the quantum dynamics of Davydov solitons in protein α -helices

Danko D. Georgiev^{a,*}, James F. Glazebrook^b

^a*Institute for Advanced Study, Varna, Bulgaria*

^b*Department of Mathematics and Computer Science, Eastern Illinois University, Charleston, IL, USA*

Abstract

The transport of energy inside protein α -helices is studied by deriving a system of quantum equations of motion from the Davydov Hamiltonian with the use of the Schrödinger equation and the generalized Ehrenfest theorem. Numerically solving the system of quantum equations of motion for different initial distributions of the amide I energy over the peptide groups confirmed the generation of both moving or stationary Davydov solitons. In this simulation the soliton generation, propagation, and stability were found to be dependent on the symmetry of the exciton-phonon interaction Hamiltonian and the initial site of application of the exciton energy.

Keywords: Davydov soliton, numerical simulation, protein α -helix, quantum dynamics, stability

1. Introduction

Proteins are the molecular engines of life that catalyze a myriad of biochemical processes in living organisms [1–3]. The physical mechanisms for transport of energy inside proteins have been of great interest to scientists ever since the discovery of the protein secondary structure in 1951 by L. Pauling and colleagues [4]. In 1973, the pioneering work of A. S. Davydov suggested that the energy released by adenosine triphosphate (ATP) could be used to excite amide I oscillators in protein α -helices, which then interact with the induced distortion in a phonon lattice to self-trap the amide I energy from dispersing thereby forming a waveform of ‘soliton’ type [5–11]. Davydov’s model has been intensively studied by different research teams [12–39], but a number of biologically important questions remained unclear, namely, whether the approximations in deriving the nonlinear Schrödinger equation [9, 25, 30, 33] for Davydov solitons in proteins are justified for short protein α -helices that enter into the tertiary structure of most proteins, and whether the system of coupled differential equations modeling the dynamics of amide I excitons and the corresponding lattice distortions are able to capture correctly the quantum nature of Davydov solitons, or the approximations involved compel the system into a purely classical regime [35, 37, 38].

Here, we investigate both of the above questions: Firstly, to an extent following [21, 22], we derive the quantum equations of motion resulting from solving the Schrödinger equation for Davydov’s Hamiltonian, followed by an application of the generalized Ehrenfest theorem for regulating the time evolution of quantum expectation values. Then (in §4) as a further mainstay of the present paper, we present a computational study of the dynamics of the Davydov solitons in protein α -helices, for the case of 40 peptide groups per α -helix spine, including the size of the conformational changes induced in the lattice, the velocity of soliton propagation and its stability upon reflection from the ends of the protein α -helix. The subsequent simulations, as depicted, reveal soliton dynamics for both symmetric and asymmetric Hamiltonians.

*Corresponding author

Email addresses: danko.georgiev@mail.bg (Danko D. Georgiev), jfglazebrook@eiu.edu (James F. Glazebrook)

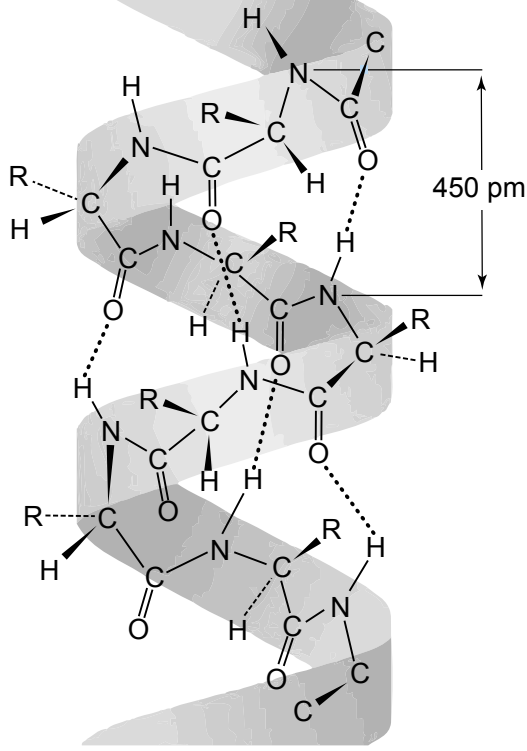
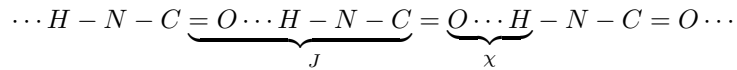


Figure 1: The protein α -helix structure is stabilized by 3 chains of hydrogen bonds referred to as α -helix spines that run parallel to the helical axis.

2. Davydov's Hamiltonian

Geometrically, the protein α -helix is a right-handed spiral with 3.6 amino acid residues per turn, where the N-H group of an amino acid forms a hydrogen bond with the C=O group of the amino acid four residues positioned earlier in the polypeptide chain. Three longitudinal chains of hydrogen bonds referred to as α -helix spines that run parallel to the helical axis stabilize the α -helix structure (Fig. 1). Each α -helix spine consists of a chain of hydrogen bonded peptide groups



where J is the interaction energy between two consecutive C=O groups, and χ is the nonlinear coupling between the excited C=O group and the distortion of the adjacent hydrogen bonds.

Focusing upon a single α -helix spine, we decompose Davydov's Hamiltonian as a sum of three separate Hamiltonians

$$\hat{H} = \hat{H}_{\text{ex}} + \hat{H}_{\text{ph}} + \hat{H}_{\text{int}} \quad (1)$$

The above Hamiltonian is formally similar to the Fröhlich-Holstein Hamiltonian which describes the interaction of electrons with a lattice [40–43].

The exciton (amide I; C=O stretching) energy operator is [11, 44]

$$\hat{H}_{\text{ex}} = \sum_n [E_0 \hat{a}_n^\dagger \hat{a}_n - J (\hat{a}_n^\dagger \hat{a}_{n+1} + \hat{a}_n^\dagger \hat{a}_{n-1})] \quad (2)$$

where \hat{a}_n^\dagger and \hat{a}_n are respectively the boson creation and annihilation operators for the amide I oscillators, $n \in \{1, 2, \dots, N\}$ counts the peptide groups along the spine, $E_0 = 3.28 \times 10^{-20}$ J is the amide-I site energy, and $J = 1.55 \times 10^{-22}$ J is the nearest neighbor dipole-dipole coupling energy along the α -helix spine [45, 46].

The phonon energy operator is [11, 21, 44]

$$\hat{H}_{\text{ph}} = \frac{1}{2} \sum_n \left[\frac{\hat{p}_n^2}{M} + w (\hat{u}_{n+1} - \hat{u}_n)^2 \right] \quad (3)$$

where $M = 1.9 \times 10^{-25}$ kg is the average mass of an amino acid, $w=13-19.5$ N/m is an effective elasticity coefficient of the lattice (the spring constant of the hydrogen bond)[44], \hat{p}_n and \hat{u}_n are respectively the momentum and position operators for longitudinal displacement of an amino acid.

The exciton-phonon interaction operator is

$$\hat{H}_{\text{int}} = \sum_n \chi (\hat{u}_{n+1} + (\xi - 1) \hat{u}_n - \xi \hat{u}_{n-1}) \hat{a}_n^\dagger \hat{a}_n \quad (4)$$

where $\chi = 30 - 62 \times 10^{-12}$ N is an anharmonic parameter arising from the coupling between the quasiparticle (exciton) and the lattice displacements (phonon) thereby parameterizing the strength of the exciton-phonon interaction [44]. Here, we have introduced the parameter $\xi = [0, 1]$ in order to characterize compactly the symmetry of the coupling between the excited C=O group and the adjacent hydrogen bonds. For example, Davydov's original spatially symmetric model is obtained for $\xi = 1$, where $\hat{a}_n^\dagger \hat{a}_n$ is coupled equally to \hat{u}_{n+1} and \hat{u}_{n-1} [11, 21]. A. C. Scott modified Davydov's model by opting for an asymmetric coupling with $\xi = 0$, motivated by the internal geometry of the peptide units such that every unit has its C=O group immediately adjacent to the next hydrogen bond in the chain; hence $\hat{a}_n^\dagger \hat{a}_n$ is coupled to \hat{u}_{n+1} , but not to \hat{u}_{n-1} [44]. Our generalized interaction Hamiltonian can be brought into the form [32] given by Luo and Piette

$$\hat{H}_{\text{int}} = \sum_n \bar{\chi} [(1 + \beta) \hat{u}_{n+1} - 2\beta \hat{u}_n - (1 - \beta) \hat{u}_{n-1}] \hat{a}_n^\dagger \hat{a}_n \quad (5)$$

where $\beta = \frac{1-\xi}{1+\xi}$ and $\bar{\chi} = \chi \frac{1+\xi}{2}$, or in terms of left χ_l and right χ_r coupling parameters, $\beta = \frac{\chi_r - \chi_l}{\chi_r + \chi_l}$, $\bar{\chi} = \frac{\chi_r + \chi_l}{2}$, $\chi = \chi_r$ and $\xi = \frac{\chi_l}{\chi_r}$.

3. Equations of motion for Davydov's Hamiltonian

Here we show how the quantum equations of motion for Davydov's Hamiltonian can be derived using only the Schrödinger equation together with the generalized Ehrenfest theorem [21, 22].

First, we introduce an ansatz state vector whose time evolution is assumed to be approximately the same as that of the exact state vector. In the literature, Davydov introduced two different possible state vectors called $|D_1\rangle$ or $|D_2\rangle$ ansätze. Because Davydov's Hamiltonian describing the transport of acoustic polarons is mathematically similar to the Holstein Hamiltonian describing optical polarons, the two Davydov ansätze and the mathematical techniques employed in the analysis of Davydov's soliton are also often used to study polaron dynamics in molecular rings and other aggregates [47, 48]. Here, we work with the second of Davydov's ansatz state vectors, which has the form [11]:

$$|D_2(t)\rangle = |a\rangle|b\rangle; \quad |a\rangle = \sum_n a_n(t) \hat{a}_n^\dagger |0_{\text{ex}}\rangle; \quad |b\rangle = e^{-\frac{i}{\hbar} \sum_j (b_j(t) \hat{p}_j - c_j(t) \hat{u}_j)} |0_{\text{ph}}\rangle \quad (6)$$

Normalization of the $|D_2\rangle$ ansatz implies $\langle D_2 | D_2 \rangle = \sum_n |a_n|^2 = 1$, where $|a_n|^2$ is the probability for finding the amide I quantum exciton at the n th site.

With the use of the Hadamard lemma [49, p. 143], the expectation values for \hat{u}_n and \hat{p}_n are found to be

$$b_n(t) = \langle D_2(t) | \hat{u}_n | D_2(t) \rangle; \quad c_n(t) = \langle D_2(t) | \hat{p}_n | D_2(t) \rangle \quad (7)$$

If the $|D_2(t)\rangle$ ansatz approximates well the exact solution of the Schrödinger equation (see Appendix B), then its temporal evolution will be

$$i\hbar \frac{d}{dt} |D_2(t)\rangle = \hat{H} |D_2(t)\rangle \quad (8)$$

and we can use the generalized Ehrenfest theorem (see Appendix A) for the time dynamics of the expectation values (7), namely

$$\frac{d}{dt}b_n = \frac{1}{i\hbar}\langle[\hat{u}_n, \hat{H}]\rangle; \quad \frac{d}{dt}c_n = \frac{1}{i\hbar}\langle[\hat{p}_n, \hat{H}]\rangle \quad (9)$$

For the above commutators, we obtain

$$[\hat{u}_n, \hat{H}] = i\hbar\frac{\hat{p}_n}{M} \quad (10)$$

$$[\hat{p}_n, \hat{H}] = i\hbar w(\hat{u}_{n+1} - 2\hat{u}_n + \hat{u}_{n-1}) - i\hbar\chi(\hat{a}_{n-1}^\dagger\hat{a}_{n-1} + (\xi - 1)\hat{a}_n^\dagger\hat{a}_n - \xi\hat{a}_{n+1}^\dagger\hat{a}_{n+1}) \quad (11)$$

From (9) and (10), we also have

$$\frac{d}{dt}b_n = \frac{c_n}{M}; \quad \frac{d}{dt}c_n = M\frac{d^2}{dt^2}b_n \quad (12)$$

From (9) and (11), together with (7) and 12, we obtain one of Davydov's equations for the phonon displacements $b_n(t)$ from the corresponding equilibrium positions

$$M\frac{d^2}{dt^2}b_n = w(b_{n+1} - 2b_n + b_{n-1}) + \chi(\xi|a_{n+1}|^2 + (1 - \xi)|a_n|^2 - |a_{n-1}|^2) \quad (13)$$

The equation for the amide I probability amplitudes $a_n(t)$ can be derived by differentiating the $|D_2(t)\rangle$ ansatz. After application of the Baker-Campbell-Hausdorff formula [50], the total time derivative of the Davydov ansatz $|D_2(t)\rangle$ is found to be [21]

$$i\hbar\frac{d}{dt}|D_2(t)\rangle = i\hbar\sum_n\frac{da_n}{dt}\hat{a}_n^\dagger|0_{\text{ex}}\rangle|b\rangle + |a\rangle\sum_j\left(\frac{db_j}{dt}\hat{p}_j - \frac{dc_j}{dt}\hat{u}_j + \frac{1}{2}\left(b_j\frac{dc_j}{dt} - \frac{db_j}{dt}c_j\right)\right)|b\rangle \quad (14)$$

Next, we calculate the terms on right-hand side of the Schrödinger equation as follows

$$\hat{H}_{\text{ex}}|D_2(t)\rangle = \sum_n\left[E_0a_n - J(a_{n+1} + a_{n-1})\right]\hat{a}_n^\dagger|0_{\text{ex}}\rangle|b\rangle \quad (15)$$

$$\hat{H}_{\text{ph}}|D_2(t)\rangle = \sum_n\hat{H}_{\text{ph}}\hat{a}_n^\dagger|0_{\text{ex}}\rangle|b\rangle \quad (16)$$

$$\hat{H}_{\text{int}}|D_2(t)\rangle = \chi\sum_n a_n(t)(\hat{u}_{n+1} + (\xi - 1)\hat{u}_n - \xi\hat{u}_{n-1})\hat{a}_n^\dagger|0_{\text{ex}}\rangle|b\rangle \quad (17)$$

Then we use the Schrödinger equation to combine (14), (15), (16) and (17), and after taking the inner product with $\langle b|0_{\text{ex}}|\hat{a}_n$, we obtain

$$i\hbar\frac{da_n}{dt} = \left[E_0 + W(t) - \frac{1}{2}\sum_j\left(\frac{db_j}{dt}c_j - b_j\frac{dc_j}{dt}\right) + \chi(b_{n+1} + (\xi - 1)b_n - \xi b_{n-1})\right]a_n - J(a_{n+1} + a_{n-1}) \quad (18)$$

where the expectation value of the phonon energy has been written as $W(t) = \langle D_2|\hat{H}_{\text{ph}}|D_2\rangle$.

The first three terms in 18 are global for all a_n , namely

$$\forall a_n: \quad \gamma(t) = E_0 + W(t) - \frac{1}{2}\sum_j\left(\frac{db_j}{dt}c_j - b_j\frac{dc_j}{dt}\right) \quad (19)$$

Furthermore, because all terms in $\gamma(t)$ are real, a global phase change on the quantum probability amplitudes, namely $a_n \rightarrow \bar{a}_n e^{-\frac{i}{\hbar}\int\gamma(t)dt}$, will not change the quantum probabilities for the amide I oscillators

$$|a_n|^2 = e^{+\frac{i}{\hbar}\int\gamma(t)dt}\bar{a}_n^*\bar{a}_n e^{-\frac{i}{\hbar}\int\gamma(t)dt} = |\bar{a}_n|^2 \quad (20)$$

After the transformation and re-labeling \bar{a}_n to a_n , the system of Davydov equations becomes

$$i\hbar \frac{da_n}{dt} = \chi [b_{n+1} + (\xi - 1)b_n - \xi b_{n-1}] a_n - J(a_{n+1} + a_{n-1}) \quad (21)$$

$$M \frac{d^2 b_n}{dt^2} = w(b_{n-1} - 2b_n + b_{n+1}) - \chi \left(|a_{n-1}|^2 + (\xi - 1)|a_n|^2 - \xi |a_{n+1}|^2 \right) \quad (22)$$

4. Computational study

4.1. Model parameters

We have numerically integrated the system of Davydov equations for an 18-nm-long protein α -helix with $n = 40$ peptide groups per α -helix spine with initially unperturbed lattice of hydrogen bonds and different initial conditions for spreading of the amide I excitation. Because counting of amino acid residues in the protein primary structure starts, by definition, at the N-end of the protein, the index n denoting the peptide groups along the α -helix spine is minimal at the N-end and maximal at the C-end of the α -helix. For improving comparability with previous works [37–39], in the present simulations we have set $w = 13$ N/m and have varied the values of $\bar{\chi}$ and ξ . The error of deviation from the Schrödinger equation due to the use of $|D_2(t)\rangle$ ansatz is analyzed in Appendix B and is numerically found to be negligible in comparison to the absolute value of the gauge transformed soliton energy $|E| = |E_{\text{sol}} - E_0 - W_0|$.

4.2. Effect of initial exciton spreading

In the continuum approximation, the Davydov soliton is a sech^2 -shaped distribution of amide I energy, which is self-trapped by the induced distortion in the lattice. To investigate how the initial spreading of amide I energy affects the dynamics of Davydov solitons in the discrete case, we have compared different initial Gaussian step distributions σ of amide I energy spread over 1, 3, 5 or 7 peptide groups such that the corresponding distributions of $|a_n|^2$ were computed to be: $\{1\}$, $\{0.244, 0.512, 0.244\}$, $\{0.099, 0.24, 0.322, 0.24, 0.099\}$, $\{0.059, 0.126, 0.199, 0.232, 0.199, 0.126, 0.059\}$. Simulations with $\xi = 1$ and $\bar{\chi} = 35$ pN showed that the larger initial spreading of amide I energy generates solitons with lower energies and lower speeds: for $\sigma = 1$ the soliton energy was $E = 0$ and the soliton velocity $v = 947$ m/s (Fig. 2a); for $\sigma = 3$: $E = -1.41J$ and $v = 590$ m/s (Fig. 2b); for $\sigma = 5$: $E = -1.73J$ and $v = 324$ m/s (Fig. 2c); and for $\sigma = 7$: $E = -1.84J$ and $v = 189$ m/s (Fig. 2d). Thus, the initial spreading of amide I energy appears to stabilize the Davydov solitons by lowering of the soliton energy.

For simulations with initially unperturbed lattice, $b_n(0) = 0$ and $\frac{db_n(0)}{dt} = 0$, the soliton energy does not depend on $\bar{\chi}$ and ξ , but only on the initial spread of the amide I energy (for details see Eq. B.5 and the following discussion in Appendix B). All subsequent simulations were performed with initial Gaussian step distribution $\sigma = 3$, which was computationally confirmed to generate Davydov solitons with the same energy $E = -1.41J$.

4.3. Effect of increased exciton-phonon coupling

To investigate how the change of the exciton-phonon coupling $\bar{\chi}$ affects the dynamics of Davydov solitons, we have varied $\bar{\chi}$ for fixed $\xi = 1$ and initial Gaussian step distribution $\sigma = 3$ of amide I energy applied at the N-end of the α -helix spine. For $\bar{\chi} = 10$ pN, the exciton energy interacted only weakly with the lattice and was rapidly dispersed along the α -helix spine (Fig. 3a, Video 1). For $\bar{\chi} = 30$ pN, the exciton energy was self-trapped by an induced distortion in the lattice and the soliton did not disperse even after reflection from the end of the α -helix spine (Fig. 3b, Video 2). The velocity of the moving soliton was $v = 679$ m/s. For $\bar{\chi} = 50$ pN, the self-trapping was more pronounced and the soliton velocity was lower, $v = 340$ m/s (Fig. 3c, Video 3). For $\bar{\chi} = 70$ pN, the self-trapping was so strong that it pinned the soliton and prevented it from moving along the α -helix spine (Fig. 3d, Video 4). Thus, the exciton-phonon coupling parameter $\bar{\chi}$ exhibits two distinct thresholds, a lower one for the formation of moving solitons and a higher one for soliton pinning.

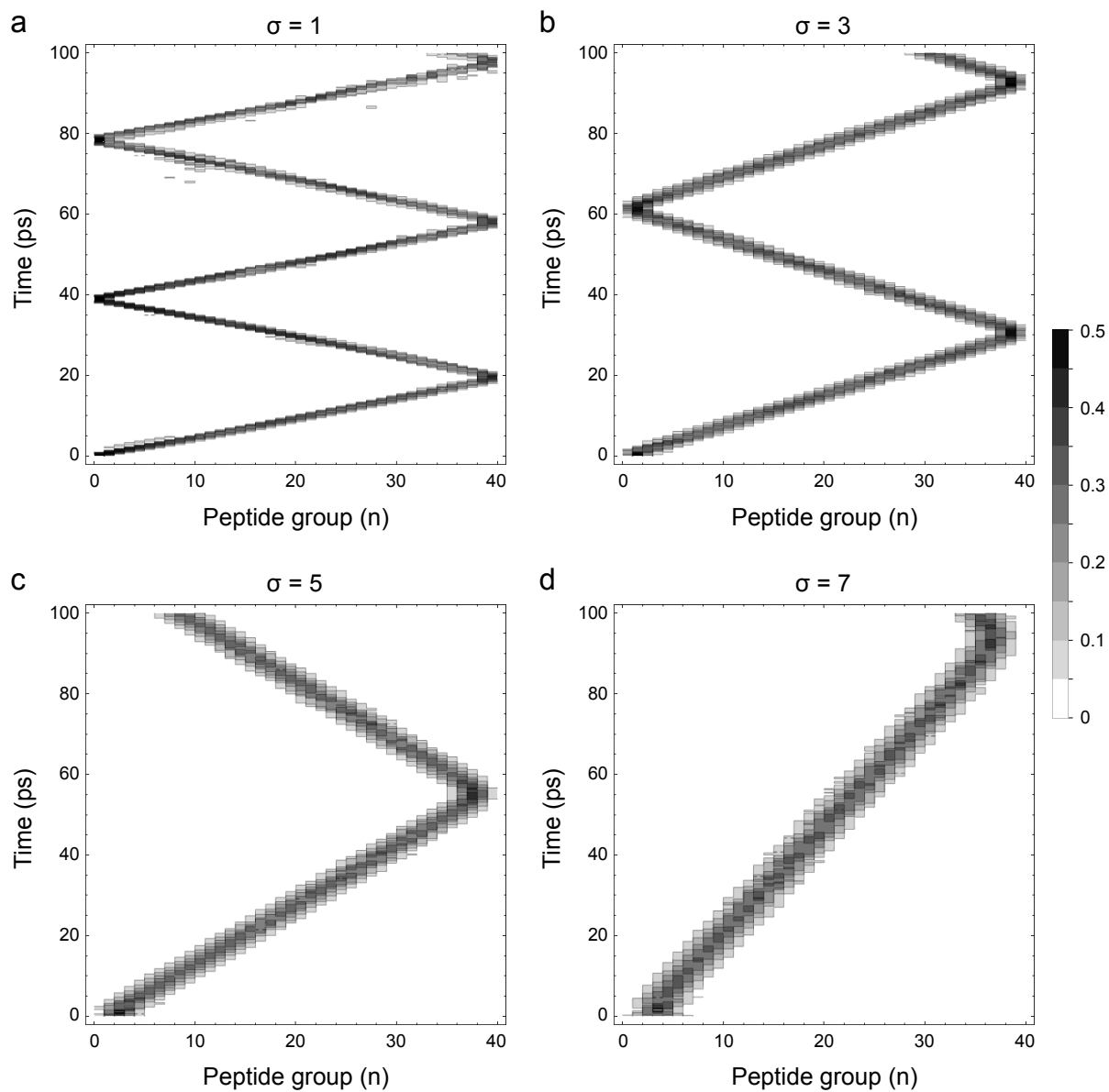


Figure 2: Soliton dynamics visualized through $|a_n|^2$ for the symmetric Hamiltonian $\xi = 1$ at supra-threshold value $\bar{\chi} = 35$ pN for different initial Gaussian step distributions σ of amide I energy over 1, 3, 5 or 7 peptide groups starting from the N-end of an α -helix spine composed of 40 peptide groups during a period of 100 ps.

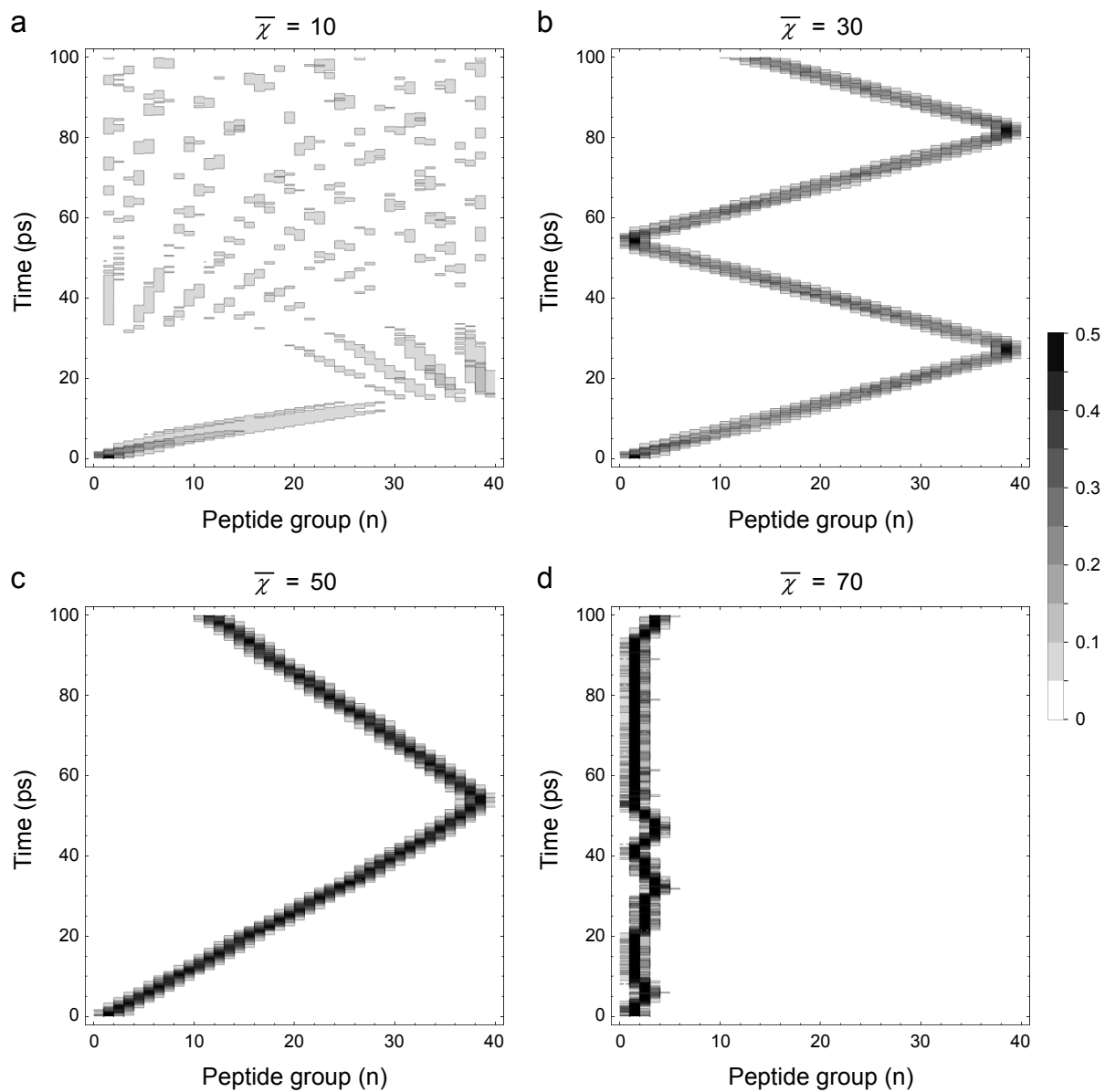


Figure 3: Soliton generation and pinning visualized through $|a_n|^2$ at different values of $\bar{\chi}$ for the symmetric Hamiltonian $\xi = 1$ with an initial Gaussian step distribution σ of amide I energy over 3 peptide groups starting from the N-end of an α -helix spine composed of 40 peptide groups during a period of 100 ps.

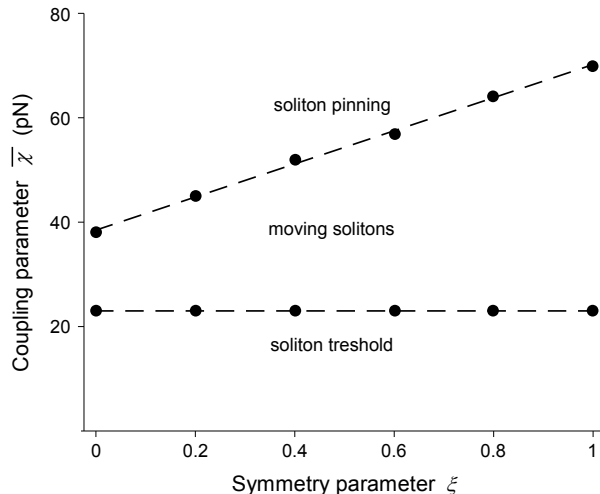


Figure 4: Thresholds for soliton generation and pinning at different values of $\bar{\chi}$ for different values of the symmetry parameter ξ with an initial Gaussian step distribution σ of amide I energy over 3 peptide groups starting from the N-end of an α -helix spine composed of 40 peptide groups during a period of 100 ps. Linear trend lines (dashed lines) are fitted to the values observed in the simulations (black circles).

4.4. Effect of exciton-phonon interaction symmetry

To investigate how the exciton-phonon interaction symmetry ξ affects the dynamics of Davydov solitons, we have varied both ξ and $\bar{\chi}$ for fixed initial distribution $\sigma = 3$. If the amide I energy was applied at the N-end of the α -helix spine, the threshold for generation of moving solitons was $\bar{\chi} = 23$ pN for any ξ (Fig. 4). This threshold is consistent with the one reported in previous simulations for $\xi = 0$ [39, 51]. Gaussians with larger initial spread, exhibited slightly lower thresholds for soliton generation: $\bar{\chi} = 22$ pN for $\sigma = 5$ and $\bar{\chi} = 21$ pN for $\sigma = 7$. Thus, launching of the Davydov solitons is modestly assisted by the initial spreading of the amide I energy.

While the threshold for soliton generation was the same for all ξ , the threshold for soliton pinning was strongly dependent on ξ . With fixed $\sigma = 3$, the thresholds for soliton pinning were: for $\xi = 0$: $\bar{\chi} = 38$ pN, for $\xi = 0.2$: $\bar{\chi} = 45$ pN, for $\xi = 0.4$: $\bar{\chi} = 52$ pN, for $\xi = 0.6$: $\bar{\chi} = 57$ pN, for $\xi = 0.8$: $\bar{\chi} = 64$ pN, and for $\xi = 1$: $\bar{\chi} = 70$ pN (Fig. 4). Thus, the symmetry of the exciton-phonon interaction Hamiltonian increases the dynamic range of $\bar{\chi}$ values for which the generated solitons are able to move along the protein α -helix.

Higher values for the symmetry parameter ξ also led to faster moving solitons. With fixed $\sigma = 3$ and $\bar{\chi} = 35$ pN, the soliton velocities were: for $\xi = 0$: $v = 340$ m/s (Fig. 5a), for $\xi = 0.25$: $v = 545$ m/s (Fig. 5b), for $\xi = 0.5$: $v = 571$ m/s (Fig. 5c), for $\xi = 0.75$: $v = 586$ m/s (Fig. 5d), for $\xi = 1$: $v = 590$ m/s (Fig. 2b). Interestingly, the presence of even a small amount of symmetry ($\xi = 0.25$) made the soliton properties closer to the fully symmetric case ($\xi = 1$) rather than the fully asymmetric case ($\xi = 0$).

We have further compared the launching of Davydov solitons from the N-end versus the C-end of the protein α -helix. The results for each ξ value were almost identical mirror reflections (Figs. 5 and 6). The mirror symmetry was exact for $\xi = 1$, and very slightly violated for $\xi < 1$.

Applying the amide I energy in the middle of the protein α -helix resulted in the generation of pinned solitons (Fig. 7). The threshold for soliton generation was substantially higher in comparison with launching of solitons from the α -helix ends and exhibited slight ξ -dependence. The thresholds for soliton generation were: for $\xi = 0$: $\bar{\chi} = 34$ pN, for $\xi = 0.25$: $\bar{\chi} = 36$ pN, for $\xi = 0.5$: $\bar{\chi} = 37$ pN, and for $\xi \geq 0.75$: $\bar{\chi} = 37$ pN. Thus, the exciton-phonon interaction asymmetry favors soliton pinning at lower values of $\bar{\chi}$ for all possible sites of application of the amide I energy in the α -helix.

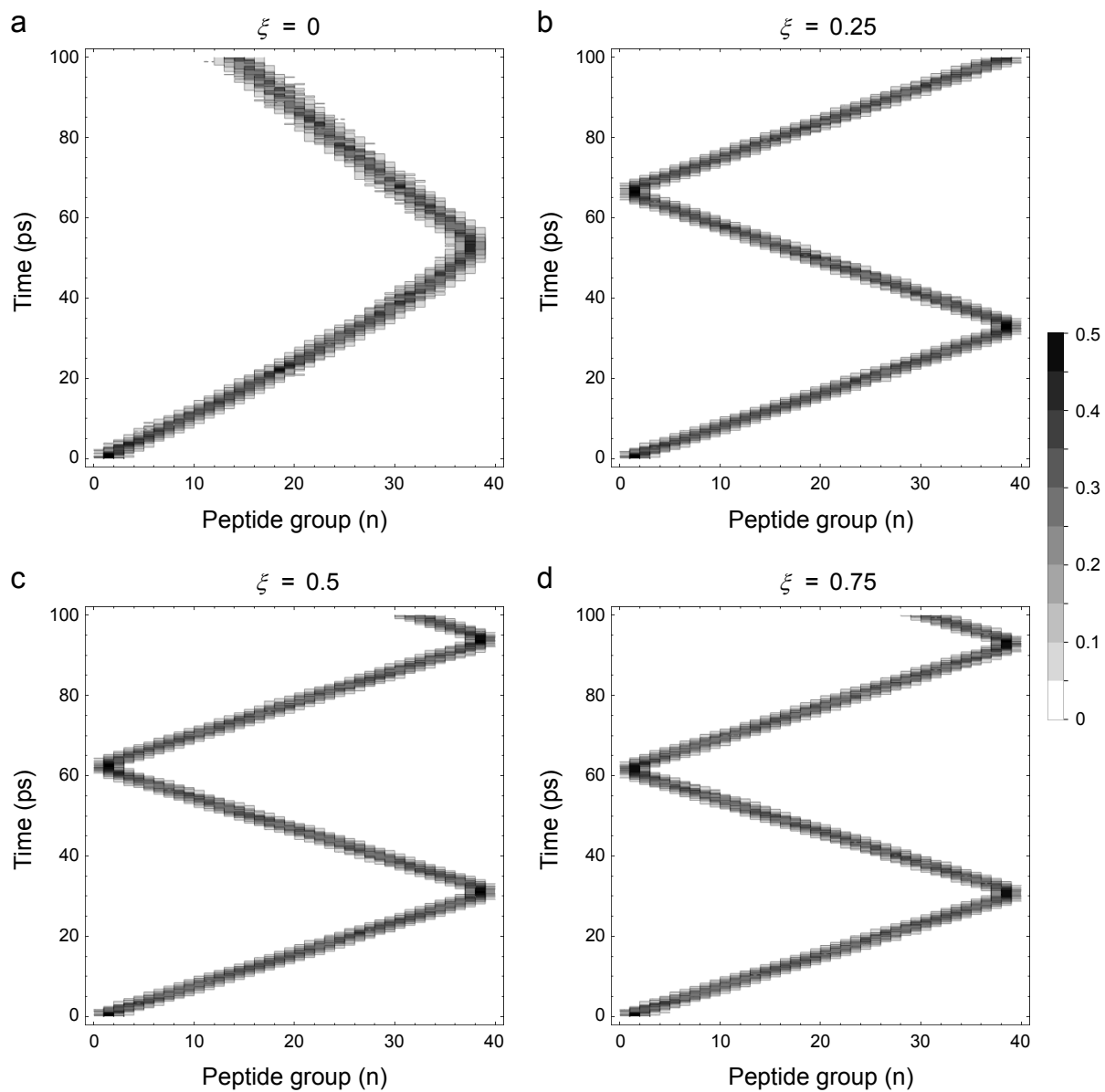


Figure 5: Soliton dynamics visualized through $|a_n|^2$ for different values of the symmetry parameter ξ at supra-threshold value $\bar{\chi} = 35$ pN with an initial Gaussian step distribution σ of amide I energy over 3 peptide groups starting from the N-end of an α -helix spine composed of 40 peptide groups during a period of 100 ps.

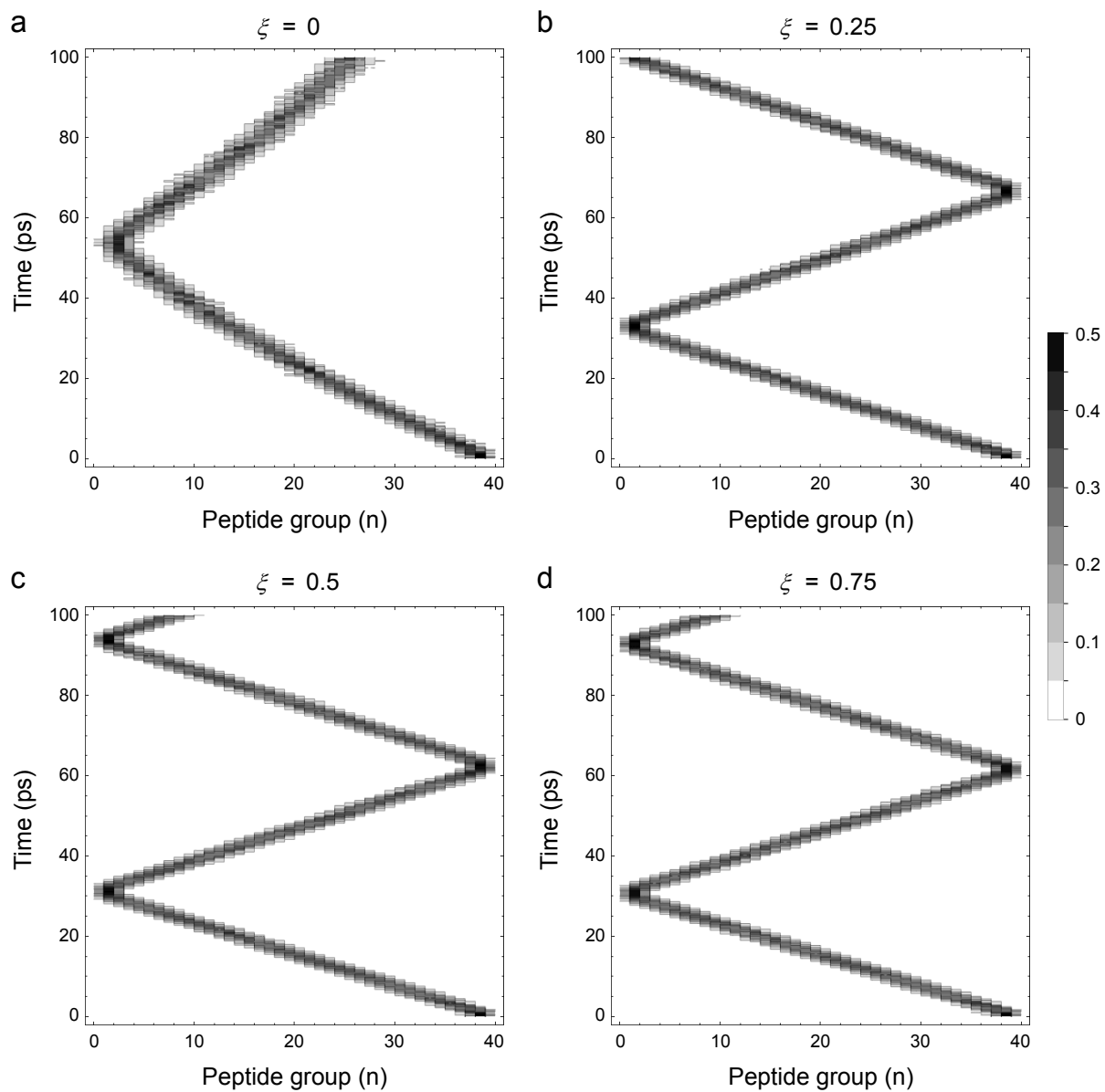


Figure 6: Soliton dynamics visualized through $|a_n|^2$ for different values of the symmetry parameter ξ at supra-threshold value $\bar{\chi} = 35$ pN with an initial Gaussian step distribution σ of amide I energy over 3 peptide groups starting from the C-end of an α -helix spine composed of 40 peptide groups during a period of 100 ps.

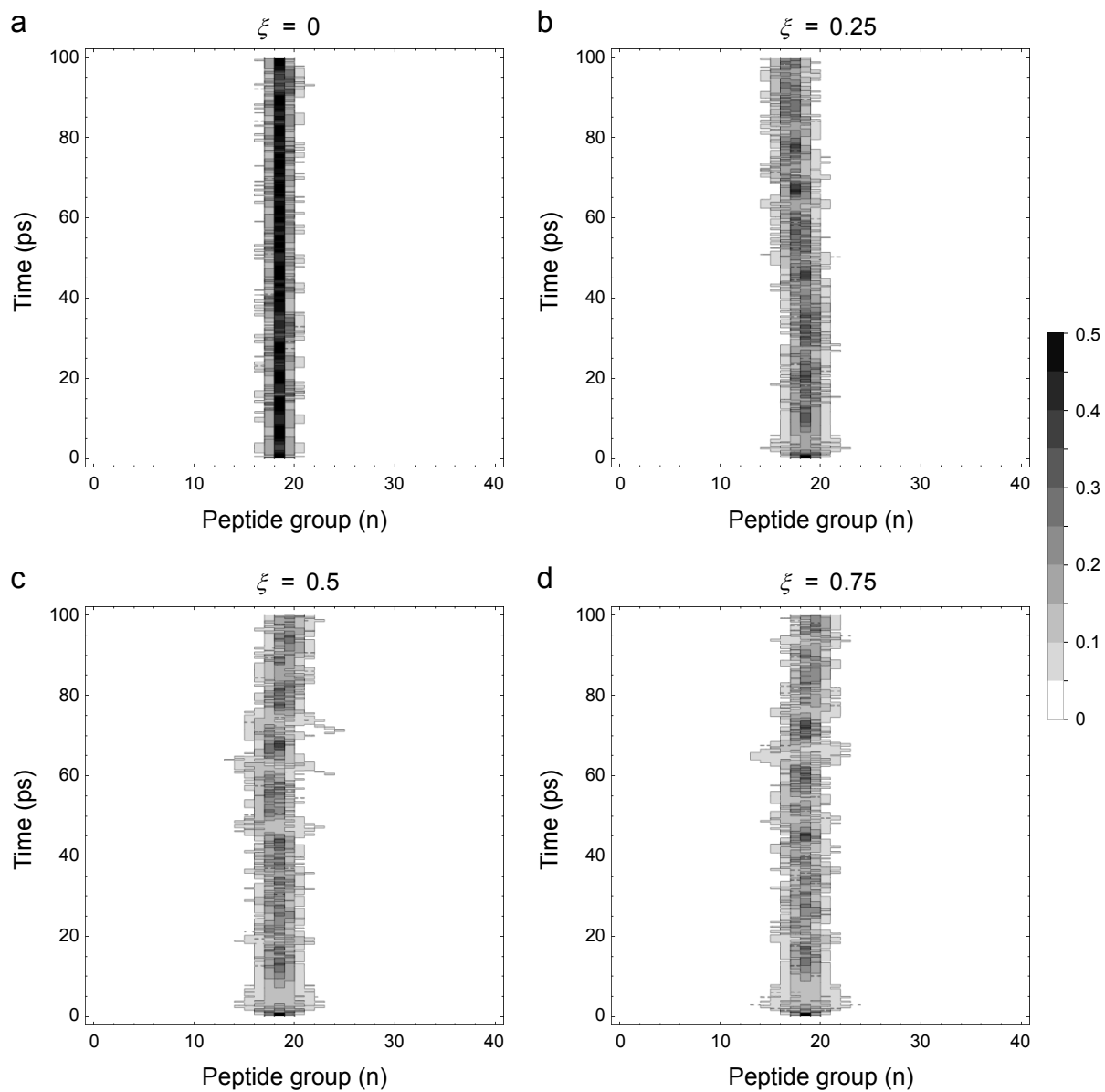


Figure 7: Soliton dynamics visualized through $|a_n|^2$ for different values of the symmetry parameter ξ at supra-threshold value $\bar{\chi} = 40$ pN with an initial Gaussian step distribution σ of amide I energy over 3 peptide groups starting in the middle of an α -helix spine composed of 40 peptide groups during a period of 100 ps.

4.5. Effect of periodic boundary conditions

Periodic boundary conditions are often used in quantum chemistry calculations [52, 53] even though they effectively create circular lattices. In a circular α -helix, the resulting solitons are pinned (Fig. 8) similarly to the case when the amide I energy is applied in the middle of the α -helix (Fig. 7). For the periodic case, the thresholds for soliton generation were slightly higher: for $\xi = 0$: $\bar{\chi} = 34$ pN, for $\xi = 0.25$: $\bar{\chi} = 37$ pN, for $\xi = 0.5$: $\bar{\chi} = 38$ pN, and for $\xi \geq 0.75$: $\bar{\chi} = 38$ pN. Thus, using periodic boundary conditions could be useful in determining the threshold for generation of solitons in the middle of the α -helix or analyzing the soliton stability, but is inadequate for studying moving solitons along the α -helix.

5. Discussion

The transport of energy in proteins is an important problem, which requires a detailed analysis of a number of physical parameters. The discreteness of the peptide groups within the relatively short lengths of average α -helices entering in the protein tertiary structure precludes the long-wavelength/continuum approximation [6, 7] with subsequent derivation of the nonlinear Schrödinger equation, which is known to have soliton solutions. With the use of the Schrödinger equation and the generalized Ehrenfest theorem, however, we have shown that it is possible to derive a system of quantum equations of motion that could be solved through numerical integration for arbitrary initial conditions. We have also addressed previous concerns [35, 36] in regard to the usage of $|D_2(t)\rangle$ ansatz for determining the full quantum dynamics by showing that the error of deviation from the Schrödinger equation is non-zero, but negligible in comparison to the soliton energy.

Different initial Gaussian step distributions σ of amide I energy exhibited self-trapping due to an associated kink in the lattice of hydrogen bonds and moved as a solitary quasiparticle (viz. Davydov soliton). The symmetry of the Hamiltonian (set by the parameter ξ) increased the dynamic range of $\bar{\chi}$ values for which the solitons were moving and also increased the soliton velocities for each individual value of $\bar{\chi}$. Furthermore, the presence of even a small amount of symmetry, makes the soliton properties closer to the fully symmetric case rather than the fully asymmetric case. Thus, any non-zero value of the symmetry parameter ξ is beneficial for the possible existence of moving Davydov solitons in protein α -helices.

Our results, as visually presented (Figs. 1–9; Videos 1–4) in the computational study (§4), show that Davydov solitons can be generated even when the long-wavelength/continuum approximation cannot be used for the derivation of the nonlinear Schrödinger equation in possession of soliton solutions. In such cases, the symmetry of the Hamiltonian is of great importance for the mobility of the generated solitons and the velocity of their propagation along the protein α -helix.

The present study, while being focused on the effects of the symmetry parameter ξ on the quantum dynamics of Davydov solitons, is limited in that it did not include a thermal bath. Consequently, the reported soliton lifetime of over 100 ps should not be directly extrapolated to physiological temperatures of $T = 310$ K. Previous experimental studies have reported self-trapped amide I states in peptide model crystals [54] or protein (myoglobin) [55] for about 15 ps. Computational studies using a quantum Monte Carlo method have found Davydov solitons to be unstable at temperatures above $T = 7$ K [56], whereas studies using a thermally averaged Hamiltonian [39] or a Langevin term obeying the fluctuation-dissipation theorem applied to the lattice [19, 20] have shown that for a certain range of parameters, Davydov solitons could persist at $T = 310$ K for tens of picoseconds. In view of this controversy, Förner [19] has pointed out that increasing the spring constant of the hydrogen bonds w is one of several promising ways to provide thermal stability of Davydov solitons because the usually used value of $w = 13$ N/m is measured in crystalline formamide [38, 57, 58], where the formamide molecules can vibrate freely against each other in the potential due to the hydrogen bonds, while in an α -helix on the contrary they are bound covalently in the backbone of the protein. Another mechanism for enhancement of thermal stability of Davydov solitons is to increase the number of amide I quanta to at least two, which corresponds to the amount of energy released by a single ATP molecule [19, 59]. Ab initio quantum chemical calculations of different parameters for the α -helix and quantum-mechanical methods that introduce the effect of thermal agitation on amide I propagation, deserve further exploration.

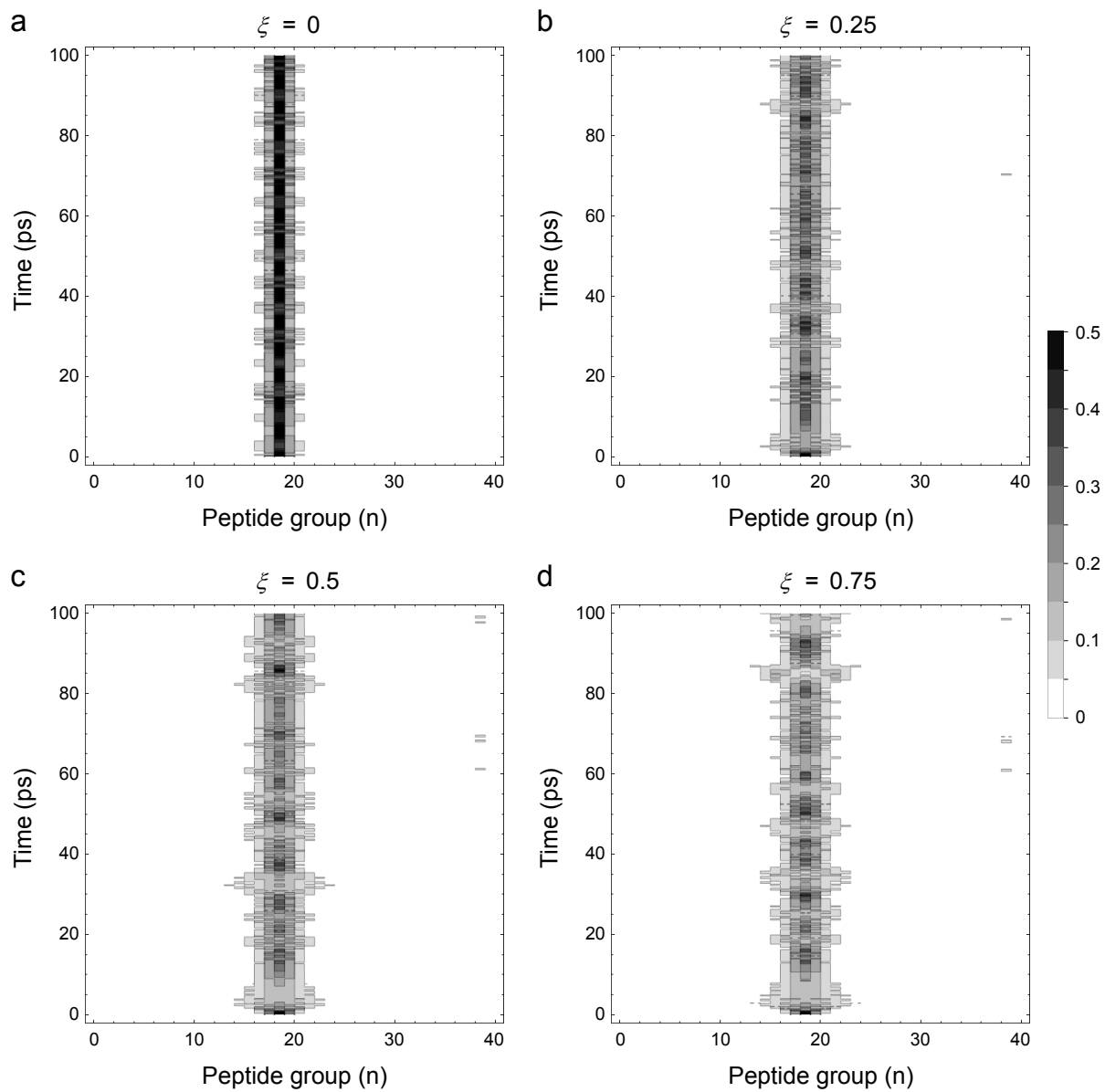


Figure 8: Soliton dynamics visualized through $|a_n|^2$ with imposed periodic boundary conditions (effectively circular α -helix spine) for different values of the symmetry parameter ξ at supra-threshold value $\bar{\chi} = 40$ pN with an initial Gaussian step distribution σ of amide I energy over 3 peptide groups in the α -helix spine composed of 40 peptide groups during a period of 100 ps.

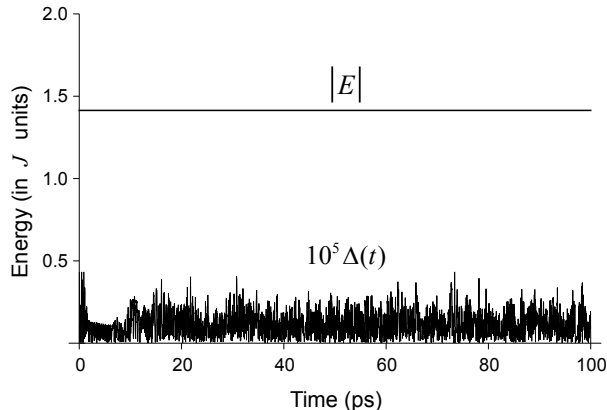


Figure 9: Numerical quantification of the error in the simulated quantum dynamics due to the use of $|D_2(t)\rangle$ ansatz for the case shown in Fig. 2b with $\xi = 1$, $\bar{\chi} = 35$ pN and $\sigma = 3$. The error $\Delta(t)$ for deviation from the Schrödinger equation is over 10^5 times smaller than the absolute value of the gauge transformed soliton energy $|E| = |E_{\text{sol}} - E_0 - W_0|$.

Conflict of interest

The authors declare that they have no conflict of interest.

Acknowledgment

We would like to thank the two anonymous reviewers for providing useful suggestions for improving the presentation of this work.

6. Supplementary videos

Video 1. Exciton dispersion at $\bar{\chi} = 10$ pN for the case shown in Fig. 3a with symmetric Hamiltonian $\xi = 1$ and an initial Gaussian step distribution σ of amide I energy over 3 peptide groups starting from the N-end of an α -helix spine composed of 40 peptide groups (extending along the x -axis) during a period of 100 ps. Quantum probabilities $|a_n|^2$ are plotted in blue along the z -axis. Phonon lattice displacement differences $b_n - b_{n-1}$ (measured in picometers) are plotted in red along the y -axis.

Video 2. Moving soliton at $\bar{\chi} = 30$ pN for the case shown in Fig. 3b with symmetric Hamiltonian $\xi = 1$ and an initial Gaussian step distribution σ of amide I energy over 3 peptide groups starting from the N-end of an α -helix spine composed of 40 peptide groups (extending along the x -axis) during a period of 100 ps. Quantum probabilities $|a_n|^2$ are plotted in blue along the z -axis. Phonon lattice displacement differences $b_n - b_{n-1}$ (measured in picometers) are plotted in red along the y -axis. The soliton is formed by self-trapping of the amide I energy by the induced lattice distortion.

Video 3. Moving soliton at $\bar{\chi} = 50$ pN for the case shown in Fig. 3c with symmetric Hamiltonian $\xi = 1$ and an initial Gaussian step distribution σ of amide I energy over 3 peptide groups starting from the N-end of an α -helix spine composed of 40 peptide groups (extending along the x -axis) during a period of 100 ps. Quantum probabilities $|a_n|^2$ are plotted in blue along the z -axis. Phonon lattice displacement differences $b_n - b_{n-1}$ (measured in picometers) are plotted in red along the y -axis. The soliton is formed by self-trapping of the amide I energy by the induced lattice distortion.

Video 4. Pinned soliton at $\bar{\chi} = 70$ pN for the case shown in Fig. 3d with symmetric Hamiltonian $\xi = 1$ and an initial Gaussian step distribution σ of amide I energy over 3 peptide groups starting from the N-end of an α -helix spine composed of 40 peptide groups (extending along the x -axis) during a period of 100 ps. Quantum probabilities $|a_n|^2$ are plotted in blue along the z -axis. Phonon lattice displacement differences $b_n - b_{n-1}$ (measured in picometers) are plotted in red along the y -axis. The soliton is formed by self-trapping of the amide I energy by the induced lattice distortion.

Appendix A. The generalized Ehrenfest theorem

The generalized Ehrenfest theorem [60] follows directly from the Schrödinger equation and represents the underlying quantum dynamics. Suppose that we have an observable $\hat{A}(x, t)$ and a quantum system in a state $|\Psi(x, t)\rangle$ evolving in time. After differentiation, we have

$$\frac{d}{dt}\langle A(x, t) \rangle = \left(\frac{\partial}{\partial t} \langle \Psi | \right) \hat{A}(x, t) | \Psi \rangle + \langle \Psi | \left(\frac{\partial}{\partial t} \hat{A}(x, t) \right) | \Psi \rangle + \langle \Psi | \hat{A}(x, t) \left(\frac{\partial}{\partial t} | \Psi \rangle \right) \quad (\text{A.1})$$

The Schrödinger equation and its complex conjugate transpose are

$$\frac{\partial}{\partial t} | \Psi \rangle = -\frac{i}{\hbar} \hat{H} | \Psi \rangle; \quad \frac{\partial}{\partial t} \langle \Psi | = \frac{i}{\hbar} \langle \Psi | \hat{H} \quad (\text{A.2})$$

where we used the Hermiticity of the Hamiltonian $\hat{H} = \hat{H}^\dagger$. Substituting these equations in (A.1) gives

$$\frac{d}{dt}\langle A(x, t) \rangle = \frac{1}{i\hbar} \langle [\hat{A}(x, t), \hat{H}] \rangle + \langle \frac{\partial}{\partial t} \hat{A}(x, t) \rangle \quad (\text{A.3})$$

where $[\hat{A}(x, t), \hat{H}] = \hat{A}(x, t)\hat{H} - \hat{H}\hat{A}(x, t)$ is the commutator of $\hat{A}(x, t)$ with the Hamiltonian \hat{H} . For time independent operator \hat{A} , the expectation value of its partial time derivative is zero, $\langle \frac{\partial}{\partial t} \hat{A} \rangle = 0$, hence the last term in Eq. A.3 disappears.

Appendix B. Deviation vector of the $|D_2\rangle$ ansatz

The D_2 theorem by Brown [36] states that Davydov's $|D_2(t)\rangle$ ansatz satisfies the Schrödinger equation of the Fröhlich Hamiltonian [40, 41] if and only if $\chi = 0$. Thus, there will be some non-zero error when using $|D_2\rangle$ ansatz to study the quantum dynamics of Davydov solitons in proteins, however, Brown's theorem does not provide a measure of the deviation of the $|D_2\rangle$ ansatz from the true Schrödinger solution. To quantify the deviation from the Schrödinger equation, we follow the method by Sun *et al.* [47] and calculate the amplitude of the deviation vector $|\delta(t)\rangle$, which is defined as

$$\Delta(t) \equiv \sqrt{\langle \delta(t) | \delta(t) \rangle} \quad (\text{B.1})$$

where

$$|\delta(t)\rangle \equiv i\hbar \frac{\partial}{\partial t} |D_2(t)\rangle - \hat{H} |D_2(t)\rangle \quad (\text{B.2})$$

Because we have transformed away certain terms $\gamma(t)$ contributing a highly oscillatory pure phase to the dynamic Davydov equations, the deviation vector of the $|D_2\rangle$ ansatz is reduced to

$$|\delta(t)\rangle = \sum_n \left[i\hbar \frac{da_n}{dt} + J(a_{n+1} + a_{n-1}) - \chi a_n (\hat{u}_{n+1} + (\xi - 1)\hat{u}_n - \xi \hat{u}_{n-1}) \right] \hat{a}_n^\dagger |0_{\text{ex}}\rangle |b\rangle \quad (\text{B.3})$$

Taking the inner product further gives

$$\begin{aligned}
\langle \delta(t) | \delta(t) \rangle &= \sum_n \left[\hbar^2 \left| \frac{da_n}{dt} \right|^2 + 2\hbar J \operatorname{Im} \left[\frac{da_n^*}{dt} (a_{n+1} + a_{n-1}) \right] + J^2 |a_{n+1} + a_{n-1}|^2 \right. \\
&\quad + 2 \left\{ \hbar \chi \operatorname{Im} \left[\frac{da_n}{dt} a_n^* \right] - \chi J \operatorname{Re} [a_n^* (a_{n+1} + a_{n-1})] \right\} (b_{n+1} + (\xi - 1)b_n - \xi b_{n-1}) \\
&\quad \left. + \chi^2 |a_n|^2 (b_{n+1} + (\xi - 1)b_n - \xi b_{n-1})^2 \right] \tag{B.4}
\end{aligned}$$

In our simulations, the error for deviation from the Schrödinger equation is found to be non-zero (Fig. 9), but negligible in comparison with the soliton energy $E_{\text{sol}} = \langle D_2(t) | \hat{H} | D_2(t) \rangle$, which is

$$\begin{aligned}
E_{\text{sol}} &= E_0 + W_0 - \sum_n \left\{ 2J [\operatorname{Re}(a_n)\operatorname{Re}(a_{n+1}) + \operatorname{Im}(a_n)\operatorname{Im}(a_{n+1})] - \chi |a_n|^2 (b_{n+1} + (\xi - 1)b_n - \xi b_{n-1}) \right. \\
&\quad \left. - \frac{1}{2} M \left(\frac{db_n}{dt} \right)^2 - \frac{1}{2} w (b_{n+1} - b_n)^2 \right\} \tag{B.5}
\end{aligned}$$

where W_0 is the zero-point energy of the lattice vibrations. In the absence of a thermal bath, E_{sol} corresponds to the total energy of the system and is a conserved quantity. Because the contribution from the two constant energies $E_0 + W_0$ is two orders of magnitude larger than the remaining energy terms, in the main text we have reported the gauge transformed soliton energy $E = E_{\text{sol}} - E_0 - W_0$. The error is negligible, $\Delta(t) < 10^{-5}|E|$, for the whole dynamic range of $\bar{\chi} \leq 70$ pN including the threshold for soliton pinning, which shows that the Davydov soliton is an excellent approximation to the full quantum dynamics in the absence of thermal agitation. Thus, the $|D_2\rangle$ ansatz is dynamically equivalent to the mixed quantum-classical approach in which the lattice is considered classical [13, 51].

References

- [1] Z. Bu, D. J. E. Callaway, Proteins move! Protein dynamics and long-range allostery in cell signaling, in: R. Donez (Ed.), *Advances in Protein Chemistry and Structural Biology*, Vol. 83, Academic Press, 2011, pp. 163–221. doi:10.1016/B978-0-12-381262-9.00005-7.
- [2] H. Frauenfelder, S. G. Sligar, P. G. Wolynes, The energy landscapes and motions of proteins, *Science* 254 (5038) (1991) 1598–1603. doi:10.1126/science.1749933.
- [3] D. D. Georgiev, J. F. Glazebrook, The quantum physics of synaptic communication via the SNARE protein complex, *Progress in Biophysics and Molecular Biology* 135 (2018) 16–29. doi:10.1016/j.pbiomolbio.2018.01.006.
- [4] L. Pauling, R. B. Corey, H. R. Branson, The structure of proteins: two hydrogen-bonded helical configurations of the polypeptide chain, *Proceedings of the National Academy of Sciences* 37 (4) (1951) 205–211. doi:10.1073/pnas.37.4.205.
- [5] A. S. Davydov, The theory of contraction of proteins under their excitation, *Journal of Theoretical Biology* 38 (3) (1973) 559–569. doi:10.1016/0022-5193(73)90256-7.
- [6] A. S. Davydov, N. I. Kislukha, Solitary excitons in one-dimensional molecular chains, *Physica Status Solidi (b)* 59 (2) (1973) 465–470. doi:10.1002/pssb.2220590212.
- [7] A. S. Davydov, N. I. Kislukha, Solitons in one-dimensional molecular chains, *Physica Status Solidi (b)* 75 (2) (1976) 735–742. doi:10.1002/pssb.2220750238.
- [8] A. S. Davydov, Solitons and energy transfer along protein molecules, *Journal of Theoretical Biology* 66 (2) (1977) 379–387. doi:10.1016/0022-5193(77)90178-3.
- [9] A. S. Davydov, Solitons, bioenergetics, and the mechanism of muscle contraction, *International Journal of Quantum Chemistry* 16 (1) (1979) 5–17. doi:10.1002/qua.560160104.
- [10] A. S. Davydov, Solitons in molecular systems, *Physica Scripta* 20 (3-4) (1979) 387–394. doi:10.1088/0031-8949/20/3-4/013.
- [11] A. S. Davydov, Solitons in quasi-one-dimensional molecular structures, *Soviet Physics Uspekhi* 25 (12) (1982) 898–918. doi:10.1070/pu1982v025n12abeh005012.
- [12] P. L. Christiansen, A. C. Scott, *Davydov’s Soliton Revisited: Self-Trapping of Vibrational Energy in Protein*, NATO ASI Series, Springer, New York, 1990. doi:10.1007/978-1-4757-9948-4.
- [13] L. Cruzeiro-Hansson, S. Takeno, Davydov model: the quantum, mixed quantum-classical, and full classical systems, *Physical Review E* 56 (1997) 894–906. doi:10.1103/PhysRevE.56.894.

- [14] L. Cruzeiro, The Davydov/Scott model for energy storage and transport in proteins, *Journal of Biological Physics* 35 (1) (2009) 43–55. doi:10.1007/s10867-009-9129-0.
- [15] W. Förner, Quantum and disorder effects in Davydov soliton theory, *Physical Review A* 44 (4) (1991) 2694–2708. doi:10.1103/PhysRevA.44.2694.
- [16] W. Förner, Davydov soliton dynamics: initial state, boundary conditions, and numerical procedure, *Journal of Computational Chemistry* 13 (3) (1992) 275–313. doi:10.1002/jcc.540130304.
- [17] W. Förner, Davydov soliton dynamics in proteins: I. Initial states and exactly solvable special cases, *Journal of Molecular Modeling* 2 (5) (1996) 70–102. doi:10.1007/s0089460020070.
- [18] W. Förner, Davydov soliton dynamics in proteins: II. The general case, *Journal of Molecular Modeling* 2 (5) (1996) 103–135. doi:10.1007/s0089460020103.
- [19] W. Förner, Davydov soliton dynamics in proteins: III. Applications and calculation of vibrational spectra, *Journal of Molecular Modeling* 3 (2) (1997) 78–116. doi:10.1007/s0089470030078.
- [20] W. Förner, Davydov solitons in proteins, *International Journal of Quantum Chemistry* 64 (3) (1997) 351–377. doi:10.1002/(SICI)1097-461X(1997)64:3<351::AID-QUA7>3.0.CO;2-V.
- [21] W. C. Kerr, P. S. Lomdahl, Quantum-mechanical derivation of the equations of motion for Davydov solitons, *Physical Review B* 35 (7) (1987) 3629–3632. doi:10.1103/PhysRevB.35.3629.
- [22] W. C. Kerr, P. S. Lomdahl, Quantum-mechanical derivation of the Davydov equations for multi-quanta states, in: P. L. Christiansen, A. C. Scott (Eds.), *Davydov’s Soliton Revisited: Self-Trapping of Vibrational Energy in Protein*, Springer, New York, 1990, pp. 23–30. doi:10.1007/978-1-4757-9948-4_2.
- [23] A. F. Lawrence, J. C. McDaniel, B. C. Chang, B. M. Pierce, R. R. Birge, Dynamics of the Davydov model in α -helical proteins: effects of coupling parameters and temperature, *Physical Review A* 33 (2) (1986) 1188–1201. doi:10.1103/PhysRevA.33.1188.
- [24] A. F. Lawrence, J. C. McDaniel, D. B. Chang, R. R. Birge, The nature of phonons and solitary waves in α -helical proteins, *Biophysical Journal* 51 (5) (1987) 785–793. doi:10.1016/S0006-3495(87)83405-7.
- [25] M. Daniel, M. M. Latha, A generalized Davydov soliton model for energy transfer in alpha helical proteins, *Physica A* 298 (3-4) (2001) 351–370. doi:10.1016/S0378-4371(01)00263-1.
- [26] M. Daniel, M. M. Latha, Soliton in alpha helical proteins with interspine coupling at higher order, *Physics Letters A* 302 (2-3) (2002) 94–104. doi:10.1016/S0375-9601(02)01110-6.
- [27] L. Brizhik, A. Eremko, B. Piette, W. Zakrzewski, Solitons in α -helical proteins, *Physical Review E* 70 (3) (2004) 031914. doi:10.1103/PhysRevE.70.031914.
- [28] L. Brizhik, A. Eremko, B. Piette, W. Zakrzewski, Charge and energy transfer by solitons in low-dimensional nanosystems with helical structure, *Chemical Physics* 324 (1) (2006) 259–266. doi:10.1016/j.chemphys.2006.01.033.
- [29] L. Brizhik, A. Eremko, B. Piette, W. Zakrzewski, Ratchet effect of Davydov’s solitons in nonlinear low-dimensional nanosystems, *International Journal of Quantum Chemistry* 110 (1) (2010) 25–37. doi:10.1002/qua.22083.
- [30] A. Biswas, A. Moran, D. Milovic, F. Majid, K. C. Biswas, An exact solution for the modified nonlinear Schrödinger’s equation for Davydov solitons in α -helix proteins, *Mathematical Biosciences* 227 (1) (2010) 68–71. doi:10.1016/j.mbs.2010.05.008.
- [31] B. LeMesurier, Studying Davydov’s ODE model of wave motion in α -helix protein using exactly energymomentum conserving discretizations for Hamiltonian systems, *Mathematics and Computers in Simulation* 82 (7) (2012) 1239–1248. doi:10.1016/j.matcom.2010.11.017.
- [32] J. Luo, B. Piette, A generalised Davydov-Scott model for polarons in linear peptide chains, *European Physical Journal B* 90 (8) (2017) 155. doi:10.1140/epjb/e2017-80209-2.
- [33] N. Taghizadeh, Q. Zhou, M. Ekici, M. Mirzazadeh, Soliton solutions for Davydov solitons in α -helix proteins, *Superlattices and Microstructures* 102 (2017) 323–341. doi:10.1016/j.spmi.2016.12.057.
- [34] L. G. Blyakhman, E. M. Gromov, I. V. Onosova, V. V. Tyutin, Dynamics of the DavydovScott soliton with location or velocity mismatch of its high-frequency component, *Physics Letters A* 381 (17) (2017) 1490–1492. doi:10.1016/j.physleta.2017.02.043.
- [35] D. W. Brown, B. J. West, K. Lindenberg, Davydov solitons: new results at variance with standard derivations, *Physical Review A* 33 (6) (1986) 4110–4120. doi:10.1103/PhysRevA.33.4110.
- [36] D. W. Brown, Balancing the Schrödinger equation with Davydov ansätze, *Physical Review A* 37 (12) (1988) 5010–5011. doi:10.1103/PhysRevA.37.5010.
- [37] L. MacNeil, A. C. Scott, Launching a Davydov soliton: II. Numerical studies, *Physica Scripta* 29 (3) (1984) 284–287. doi:10.1088/0031-8949/29/3/017.
- [38] A. C. Scott, Launching a Davydov soliton: I. Soliton analysis, *Physica Scripta* 29 (3) (1984) 279–283. doi:10.1088/0031-8949/29/3/016.
- [39] L. Cruzeiro, J. Halding, P. L. Christiansen, O. Skovgaard, A. C. Scott, Temperature effects on the Davydov soliton, *Physical Review A* 37 (3) (1988) 880–887. doi:10.1103/PhysRevA.37.880.
- [40] H. Fröhlich, Interaction of electrons with lattice vibrations, *Proceedings of the Royal Society of London. Series A. Mathematical and Physical Sciences* 215 (1122) (1952) 291–298. doi:10.1098/rspa.1952.0212.
- [41] H. Fröhlich, Electrons in lattice fields, *Advances in Physics* 3 (11) (1954) 325–361. doi:10.1080/00018735400101213.
- [42] T. Holstein, Studies of polaron motion: Part I. The molecular-crystal model, *Annals of Physics* 8 (3) (1959) 325–342. doi:10.1016/0003-4916(59)90002-8.
- [43] T. Holstein, Studies of polaron motion: Part II. The “small” polaron, *Annals of Physics* 8 (3) (1959) 343–389. doi:10.1016/0003-4916(59)90003-X.
- [44] A. C. Scott, Davydov’s soliton, *Physics Reports* 217 (1) (1992) 1–67. doi:10.1016/0370-1573(92)90093-F.

- [45] J. M. Hyman, D. W. McLaughlin, A. C. Scott, On Davydov's alpha-helix solitons, *Physica D* 3 (1-2) (1981) 23–44. doi:10.1016/0167-2789(81)90117-2.
- [46] N. A. Nevskaya, Y. N. Chirgadze, Infrared spectra and resonance interactions of amide-I and II vibrations of α -helix, *Biopolymers* 15 (4) (1976) 637–648. doi:10.1002/bip.1976.360150404.
- [47] J. Sun, B. Luo, Y. Zhao, Dynamics of a one-dimensional Holstein polaron with the Davydov ansätze, *Physical Review B* 82 (1) (2010) 014305. doi:10.1103/PhysRevB.82.014305.
- [48] K. Sun, J. Ye, Y. Zhao, Path induced coherent energy transfer in light-harvesting complexes in purple bacteria, *Journal of Chemical Physics* 141 (12) (2014) 124103. doi:10.1063/1.4895791.
- [49] W. P. Bowen, G. J. Milburn, *Quantum Optomechanics*, CRC Press, Boca Raton, 2015. doi:10.1201/b19379.
- [50] A. Van-Brunt, M. Visser, Special-case closed form of the Baker–Campbell–Hausdorff formula, *Journal of Physics A: Mathematical and Theoretical* 48 (22) (2015) 225207. doi:10.1088/1751-8113/48/22/225207.
- [51] V. M. Kenkre, S. Raghavan, L. Cruzeiro-Hansson, Thermal stability of extended nonlinear structures related to the Davydov soliton, *Physical Review B* 49 (14) (1994) 9511–9522. doi:10.1103/PhysRevB.49.9511.
- [52] S. K. Kolev, P. S. Petkov, M. A. Rangelov, G. N. Vayssilov, Ab initio molecular dynamics of Na^+ and Mg^{2+} counterions at the backbone of RNA in water solution, *ACS Chemical Biology* 8 (7) (2013) 1576–1589. doi:10.1021/cb300463h.
- [53] S. K. Kolev, P. S. Petkov, M. A. Rangelov, D. V. Trifonov, T. I. Milenov, G. N. Vayssilov, Interaction of Na^+ , K^+ , Mg^{2+} and Ca^{2+} counter cations with RNA, *Metallomics* 10 (5) (2018) 659–678. doi:10.1039/c8mt00043c.
- [54] J. Edler, P. Hamm, Self-trapping of the amide I band in a peptide model crystal, *Journal of Chemical Physics* 117 (5) (2002) 2415–2424. doi:10.1063/1.1487376.
- [55] A. Xie, L. van der Meer, W. Hoff, R. H. Austin, Long-lived amide I vibrational modes in myoglobin, *Physical Review Letters* 84 (23) (2000) 5435–5438. doi:10.1103/PhysRevLett.84.5435.
- [56] X. Wang, D. W. Brown, K. Lindenberg, Quantum Monte Carlo simulation of the Davydov model, *Physical Review Letters* 62 (15) (1989) 1796–1799. doi:10.1103/PhysRevLett.62.1796.
- [57] K. Itoh, T. Shimanouchi, Vibrational spectra of crystalline formamide, *Journal of Molecular Spectroscopy* 42 (1) (1972) 86–99. doi:10.1016/0022-2852(72)90146-4.
- [58] A. C. Scott, Davydov solitons in polypeptides, *Philosophical Transactions of the Royal Society of London. Series A. Mathematical and Physical Sciences* 315 (1533) (1985) 423–436. doi:10.1098/rsta.1985.0049.
- [59] L. Cruzeiro-Hansson, Two reasons why the Davydov soliton may be thermally stable after all, *Physical Review Letters* 73 (21) (1994) 2927–2930. doi:10.1103/PhysRevLett.73.2927.
- [60] B. A. Lippmann, Generalized Ehrenfest theorem, *Physical Review Letters* 16 (4) (1966) 135–138. doi:10.1103/PhysRevLett.16.135.